EXCITATION AND IONIZATION BY AURORAL PROTONS

By R. H. Eather* and K. M. Burrows†

[*Manuscript received December* 23, 1965]

Summary

Height distributions are presented for the atmospheric ionization rate and Balmer radiation resulting from precipitation of auroral protons. These results have been computed assuming proton fluxes with several different energy spectra and pitch-angle distributions about the magnetic field, the total proton energy range being restricted to 1–1000 keV.

The ionization results are used to obtain height distributions of radio absorption at a frequency of 27·6 MHz. It is concluded that proton impact ionization could contribute significantly to observed auroral absorption of cosmic radio noise.

Computed Hα line profiles for observation in the magnetic zenith and horizon directions are compared with observed profiles, and proton flux parameters giving best agreement are deduced.

I. Introduction

Precipitation of protons into the atmosphere in the auroral zones is known to occur, from the observed Doppler-shifted hydrogen emission as well as from direct measurements with rocket-borne instruments. Protons seldom, if ever, supply the major portion of auroral energy (Chamberlain 1961), and there is certainly no one-to-one correspondence between the subvisual hydrogen emission and other visual auroral emissions (Eather and Jacka 1966*b*).

There is evidence, however, that ionization due to precipitating protons is a cause of slowly varying absorption of cosmic radio noise (Eather and Jacka 1966*a*). Detailed interpretation of the observed correlations between riometer observations and ground-observed hydrogen Balmer emission must commence with a study of the ionization and spectral emission likely to result from the incoming flux of protons.

Unfortunately, there is still wide uncertainty in the values of the critical parameters of the proton flux in auroral zones (total particle flux, energy spectrum, and pitch distribution about the geomagnetic field). These may all be obtained, in principle, from ground observations of luminosity–height curves and Balmer-line profiles. However, the low intensity of hydrogen emission and the diffuse form of the emitting regions makes observation of line profiles difficult and renders triangulation, necessary

* Antarctic Division, Department of External Affairs, Melbourne, and School of Physics, University of New South Wales, Kensington, N.S.W.; present address: Department of Space Science, Rice University, Houston, Texas, U.S.A.

† School of Physics, University of New South Wales, Kensington, N.S.W.

for derivation of the luminosity–height distribution, practically impossible. Thus, only direct rocket observations of the proton flux parameters or, at least, of the hydrogen emission luminosity–height distribution offer any real promise of providing a complete picture of proton precipitation. The importance of this detailed description of the proton flux is, of course, not restricted to its usefulness in interpreting observed correlations of hydrogen emission with slowly varying ionospheric absorption (SVIA) events; it is essential for the development and testing of a theory of the acceleration of protons to energies necessary to penetrate to auroral altitudes.

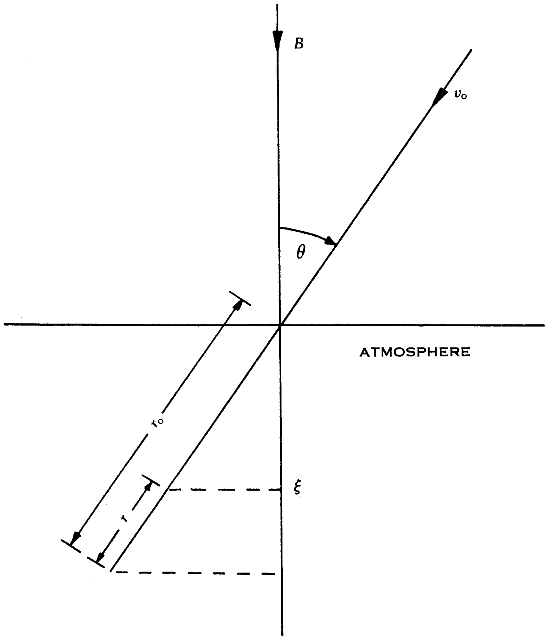

Fig. 1.—Geometry for precipitating protons. A proton with initial velocity v_0 (range r_0) enters a homogeneous atmosphere at angle θ to the magnetic field B (B assumed perpendicular to the "free surface" of the atmosphere).

Notwithstanding these uncertainties in the incoming flux characteristics, useful information can be obtained from calculation of the ionization, excitation, and radio absorption profiles, and of the magnetic zenith and horizon Balmer-line profiles, using reasonably assumed energy spectra and pitch distributions. Chamberlain (1961) and Omholt (1956) have published luminosity–height curves for monoenergetic protons, and Chamberlain has considered a particularly simple energy spectrum chosen, primarily, for simplicity of calculation. The spectra assumed here are of the type that have been obtained from rocket observations.

These calculations yield estimates of effective height and thickness of hydrogen emission zones, and they can be used as a basis for estimating the contribution to cosmic noise absorption believed to be due to proton-induced ionization.

II. Ionization by Incident Protons

The notation used here is essentially that of Chamberlain (1961), the proton flux being described by an energy spectrum expressed in terms of initial range and a pitch distribution about magnetic field lines assumed perpendicular to a plane atmosphere.

In Figure 1, r_0 is the initial proton range at the "top" of the atmosphere, r is the residual range, and ξ is the equivalent depth in a homogeneous atmosphere. All ranges are expressed in atm-cm. Following Chamberlain (1961), we consider protons spiralling around lines of force with a pitch-angle distribution

$$\eta(\theta) = \frac{n+2}{2\pi}\mathscr{F}\cos^n\theta \qquad (n \geqslant -1), \tag{1}$$

where $\mathscr{F}$ is the flux of particles across unit area normal to the magnetic field, given by

$$\mathscr{F} = 2\pi\int_0^{\frac{1}{2}\pi} \eta(\theta)\cos\theta\sin\theta\,\mathrm{d}\theta. \tag{2}$$

From Figure 1, it is seen that

$$r_0 - r = \xi\sec\theta. \tag{3}$$

Thus, with an energy spectrum of incident protons $\psi(r_0)$, $\mathscr{F}$ satisfies

$$\mathscr{F}_\xi = (n+2)\mathscr{F}\int_\xi^\infty\int_0^{r_0-\xi}\frac{\xi^{n+2}}{(r_0-r)^{n+3}}\psi(r_0)\,\mathrm{d}r\,\mathrm{d}r_0, \tag{4}$$

where $\mathscr{F}_\xi$ is the total flux of particles of all energies crossing unit area perpendicular to the magnetic field at an equivalent depth ξ.

The ionization rate per unit volume due to proton impact may be written in terms of the proton residual range as

$$q/\mathscr{F} = Cr^b\exp(-ar) \qquad \text{ion pairs per proton-cm}, \tag{5}$$

where a, b, and C are constants, evaluated by Chamberlain (1961) as

$$a = 4\cdot 63, \qquad b = 0\cdot 74, \qquad C = 2\cdot 2\times 10^5.$$

The ionization produced per unit area in the equivalent depth interval $\mathrm{d}\xi$ is proportional to $\sec\theta$; thus, using equation (4), we obtain

$$q_\xi = C(n+2)\mathscr{F}\xi^{n+1}\int_\xi^\infty\int_0^{r_0-\xi}\frac{r^b\exp(-ar)}{(r_0-r)^{n+2}}\psi(r_0)\,\mathrm{d}r\,\mathrm{d}r_0 \tag{6}$$

or, for a model atmosphere of non-uniform density, with h as the height above ground,

$$q_h = -q_\xi\frac{\mathrm{d}\xi}{\mathrm{d}h}. \tag{7}$$

III. Absorption of Cosmic Radio Noise

The equilibrium electron density N_e is given by

$$N_\mathrm{e}(h) = \left(\frac{q_h}{(1+\lambda)(\alpha_\mathrm{d}+\lambda\alpha_\mathrm{i})}\right)^{\frac{1}{2}}, \tag{8}$$

where λ is the ratio of equilibrium densities of negative ions and free electrons, at height h above ground, and α_{d} and α_{i} are the dissociative and ion–ion recombination coefficients.

The absorption of cosmic radio noise is related to the electron density by the Appleton–Hartree expression

$$\frac{\mathrm{d}A}{\mathrm{d}h} = \frac{4\cdot 59\times 10^{4} N_{\mathrm{e}}\,\nu}{3\cdot 54\times 10^{16}+\nu^{2}} \qquad \mathrm{dB/km}, \tag{9}$$

where $\mathrm{d}A$ is the attenuation in decibels over a path length $\mathrm{d}h$ and ν is the electron collision frequency at height h. The numerical constants in (9) are appropriate to the riometer frequency 27·6 MHz.

IV. The Luminosity Distribution

An empirical relation of the form (5) may, similarly, be used to represent the rate of Balmer photon emission due to electron capture and cascading. For the line Hα, Chamberlain gives the appropriate constants as

$$a' = 25\cdot 2, \qquad b' = 0\cdot 83, \qquad C' = 2\cdot 3\times 10^{4}.$$

Thus, the luminosity–equivalent-depth distribution is given by

$$F_{\xi} = C'(n+2)\mathscr{F}\,\xi^{n+1}\int_{\xi}^{\infty}\int_{0}^{r_0-\xi}\frac{r^{b'}\exp(-a'r)}{(r_0-r)^{n+2}}\,\psi(r_0)\,\mathrm{d}r\,\mathrm{d}r_0, \tag{10}$$

which may be scaled by means of (7) for application to a non-uniform atmosphere.

V. Line Profiles

Doppler profiles of Balmer emission lines reflect the velocity distribution of incoming protons about the magnetic field lines. Chamberlain (1961) has derived an expression for the total emission (in photons cm^{-2} sec^{-1} column^{-1}) due to particles spiralling down the magnetic zenith field lines with velocity component v_z in the field direction (i.e. in the line of sight), as follows:

$$4\pi I(v_z) = (n+2)\mathscr{F}\,v_z^{n+1}\int_{v_z}^{\infty}\int_{v_z}^{v_0}\frac{F(v)}{v^{n+2}}\psi(v_0)\,\mathrm{d}v\,\mathrm{d}v_0, \tag{11}$$

and, similarly, for the magnetic horizon Chamberlain obtains

$$4\pi I(v_x) = \frac{\mathscr{C}_{n+1}}{\pi}\mathscr{F}\int_{v_x}^{\infty}\int_{v_x}^{v_0}\frac{F(v)}{v^{n+2}}(v^2-v_x^2)^{\frac{1}{2}(n+1)}\psi(v_0)\,\mathrm{d}v\,\mathrm{d}v_0, \tag{12}$$

where v_x is the line-of-sight proton velocity, now normal to the field, $F(v)$ is the emission rate in terms of proton velocity, which is obtained from (10) and range–energy information, v_0 is the initial (total) proton entrance velocity, corresponding to the initial range r_0, and v is the total velocity. The function $\mathscr{C}$ is defined by Chamberlain through the relation

$$\mathscr{C}_r = (r+1)\int_0^{\frac{1}{2}\pi}\cos^r\theta\,\mathrm{d}\theta.$$

VI. Assumed Proton Flux Parameters

The relationships described above have been used as bases for the numerical computations, with the following assumed proton flux parameters.

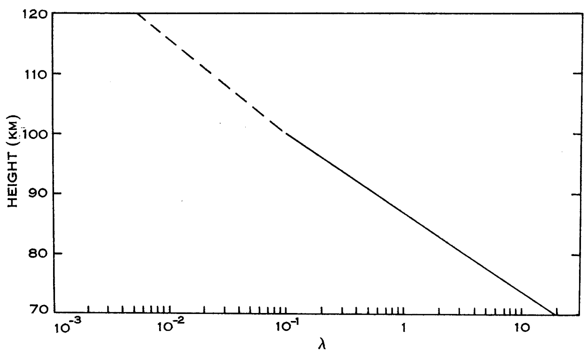

Fig. 2.—Negative ion/free electron ratio λ as a function of height in the atmosphere. ——— Aikin (1961); - - - - - extrapolation.

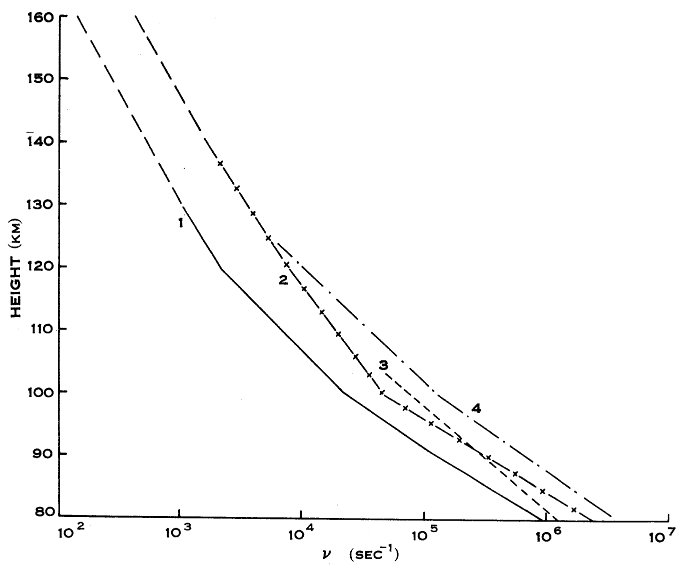

Fig. 3.—Electron collision frequency ν as a function of height in the atmosphere. 1, Ratcliffe and Weekes (1961), Holt (1963), Hultqvist (1964); 2, Nicolet (1959), Hanson (1961); 3, Fejer (1955); 4, Nicolet (1959). – – – – extrapolations.

Energy Spectrum

The energy spectrum of incoming protons is conveniently represented by an exponential function of initial energy E_0 or of initial range r_0, or by a power-law function of energy. The spectra used in these calculations were

(i) monoenergetic;

(ii) $\psi(r_0) = g\exp(-gr_0)$ with $g = 5, 10, 20, 50$;

(iii) $$\psi(E_0) = \frac{\exp(-E_0/\beta)}{\beta\{\exp(-E_{0\min}/\beta)-\exp(-E_{0\max}/\beta)\}}$$ with $\beta = 2\cdot5, 5, 10, 20, 50$;

(iv) $$\psi(E_0) = \frac{(\alpha-1)E_0^{-\alpha}}{(E_{0\min})^{1-\alpha}-(E_{0\max})^{1-\alpha}}$$ with $\alpha = 2, 3, 4$;

(v) $\psi(E_0) = \{E_0(\ln E_{0\max} - \ln E_{0\min})\}^{-1}$;

the constants $E_{0\min}$, $E_{0\max}$ in (iii), (iv), and (v) having the values

$$E_{0\min} = 1 \text{ keV}, \qquad E_{0\max} = 1 \text{ MeV}.$$

It is important to note that the absolute numerical results obtained for ionization and excitation are strongly dependent on the values chosen for $E_{0\min}$ and $E_{0\max}$.

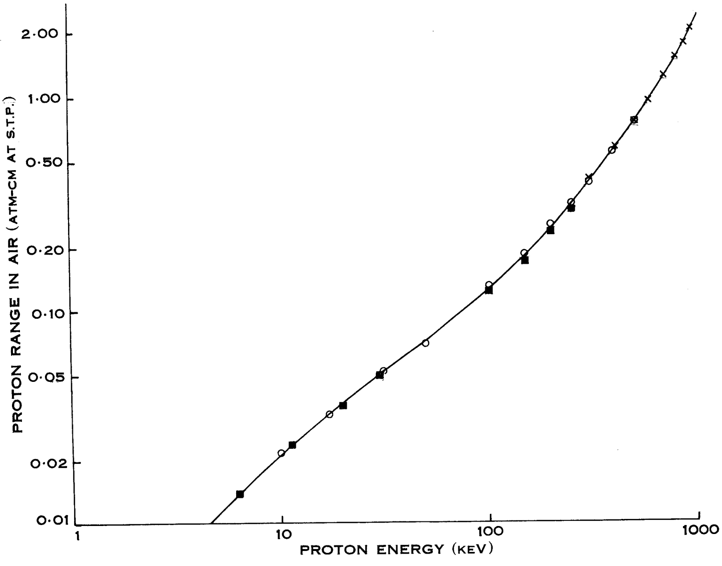

Fig. 4.—Experimental range–energy measurements for protons in air. × Jesse and Sadauskis (1950); ○ Reynolds *et al.* (1953); ■ Cook, Jones, and Jorgenson (1953).

Pitch-angle Distributions

(i) monodirectional;

(ii) isotropic;

(iii) $\eta(\theta) = \dfrac{n+2}{2\pi}\mathscr{F}\cos^n\theta$ (equation (1) above) with $n = -1$ and 2.

VII. Assumed Atmospheric Parameters

The model atmosphere described by Chamberlain (1961) has been used. For the computation of N_e from (8), the attachment profile given by Aikin (1961) has

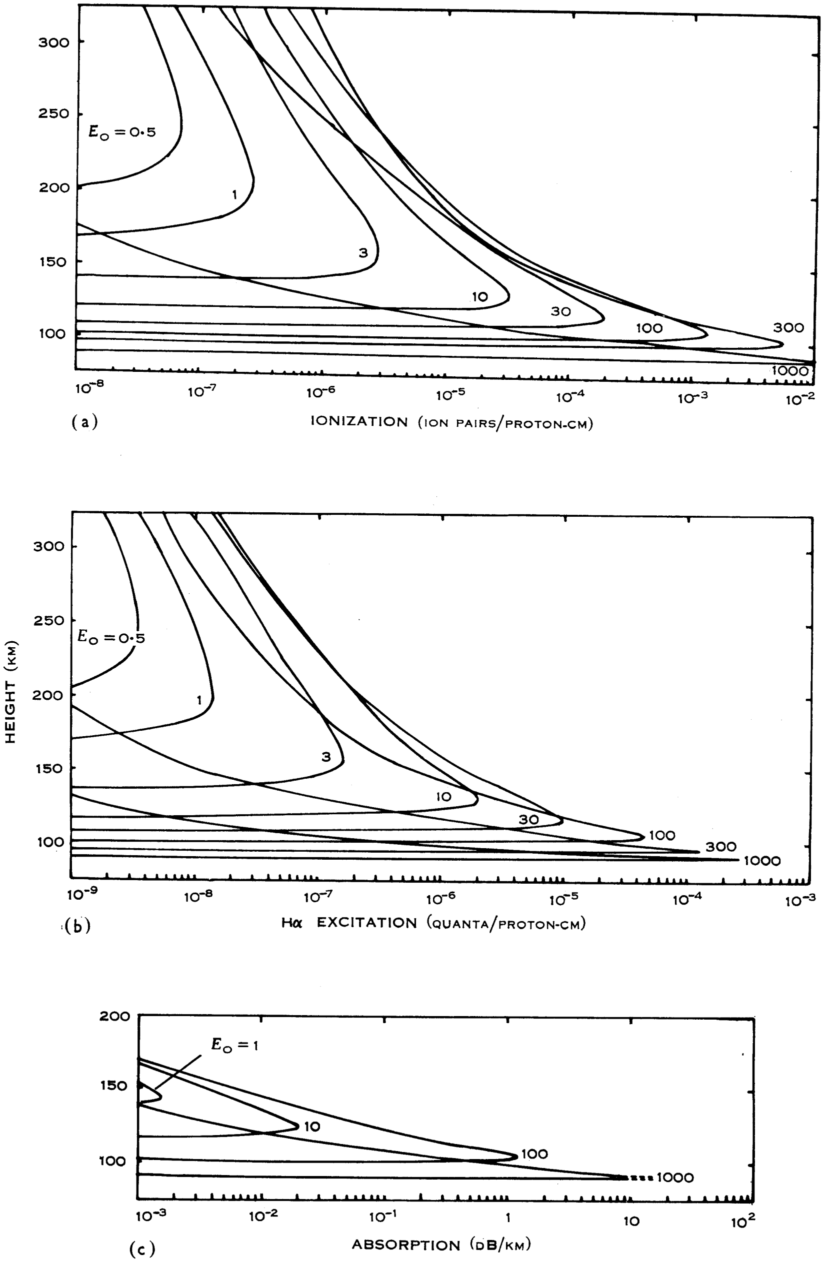

Fig. 5.—Yield profiles for monoenergetic protons with initial energies E_0 keV; isotropic angular distribution. (*a*) ionization; (*b*) Hα excitation; (*c*) absorption at 27·6 MHz for an assumed proton flux 10^6 cm^{-2} sec^{-1} sr^{-1}.

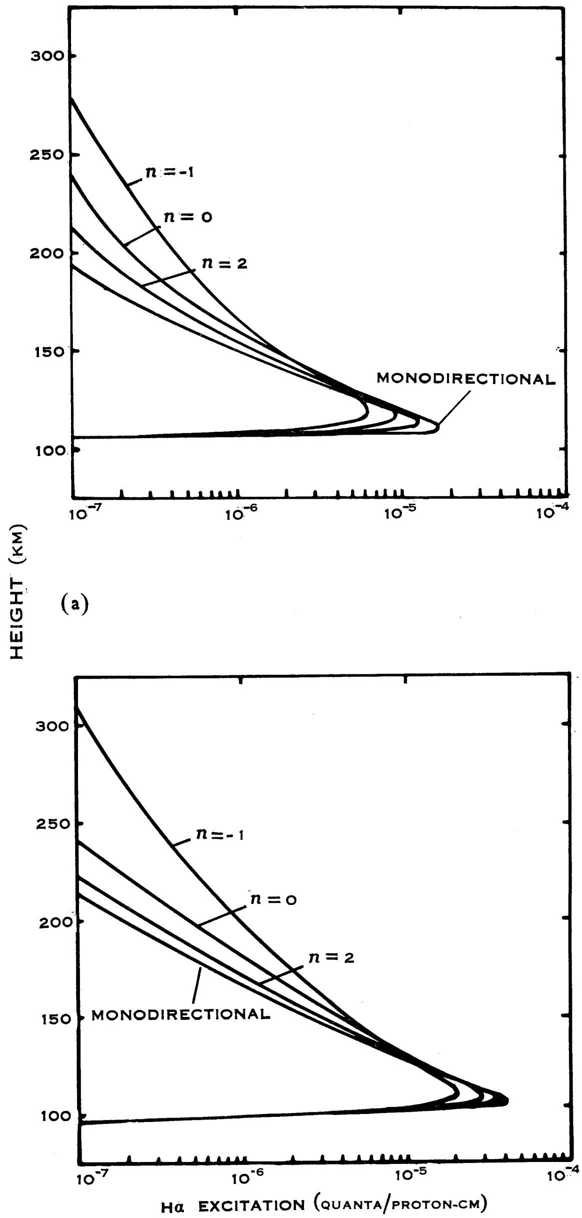

(b)

Fig. 6.—Effect of pitch-angle distribution on the Hα excitation profile. (a) monoenergetic protons with 30 keV initial energy; (b) protons distributed in energy according to the initial range spectrum $\exp(-20r_0)$. The angular distribution parameter n is as defined by equation (1).

been used to $h = 100$ km and extrapolated for higher altitudes (see Fig. 2). N_e depends only slightly on λ for heights above 100 km ($\lambda \lesssim 0 \cdot 1$), so that errors introduced by this extrapolation should not be serious.

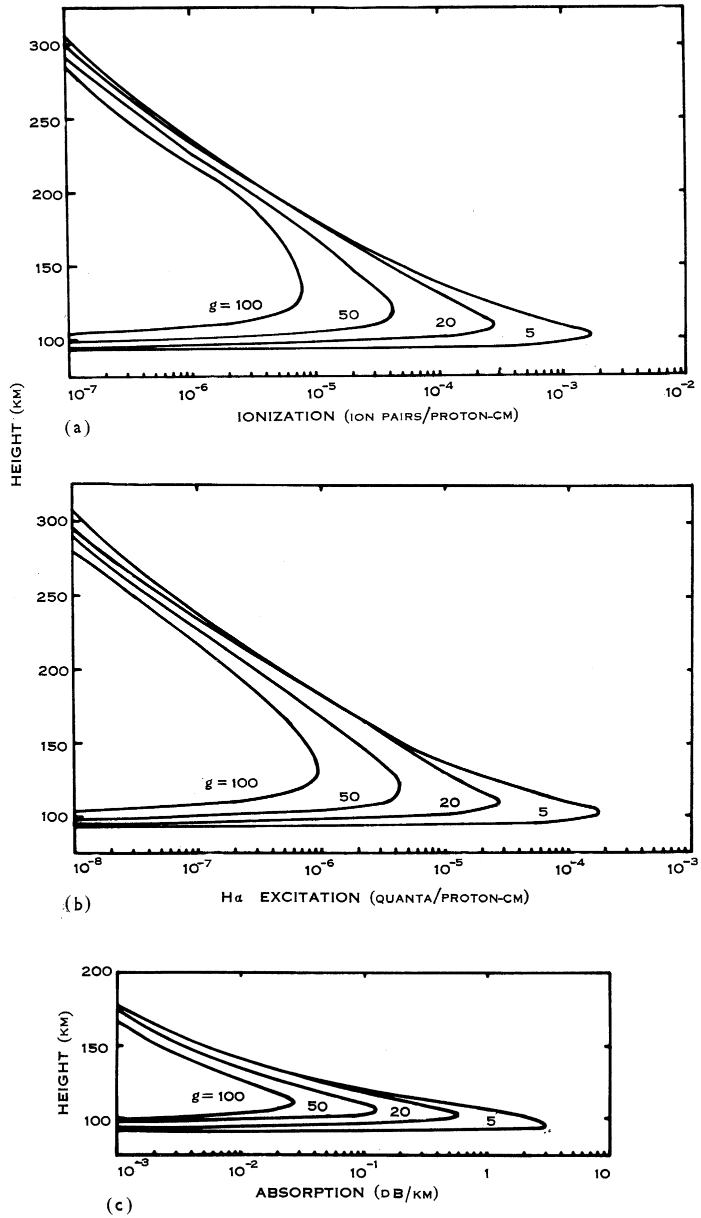

Fig. 7.—Yield profiles for protons with energies distributed according to the initial range spectra $\exp(-gr_0)$; isotropic angular distribution. (*a*) ionization; (*b*) Hα excitation; (*c*) absorption at $27 \cdot 6$ MHz for an assumed proton flux 10^6 cm^{-2} sec^{-1} sr^{-1}.

The electron collision frequency profile adopted by Hultqvist (1964) (profile 1 of Fig. 3) has been chosen from several that have been published.

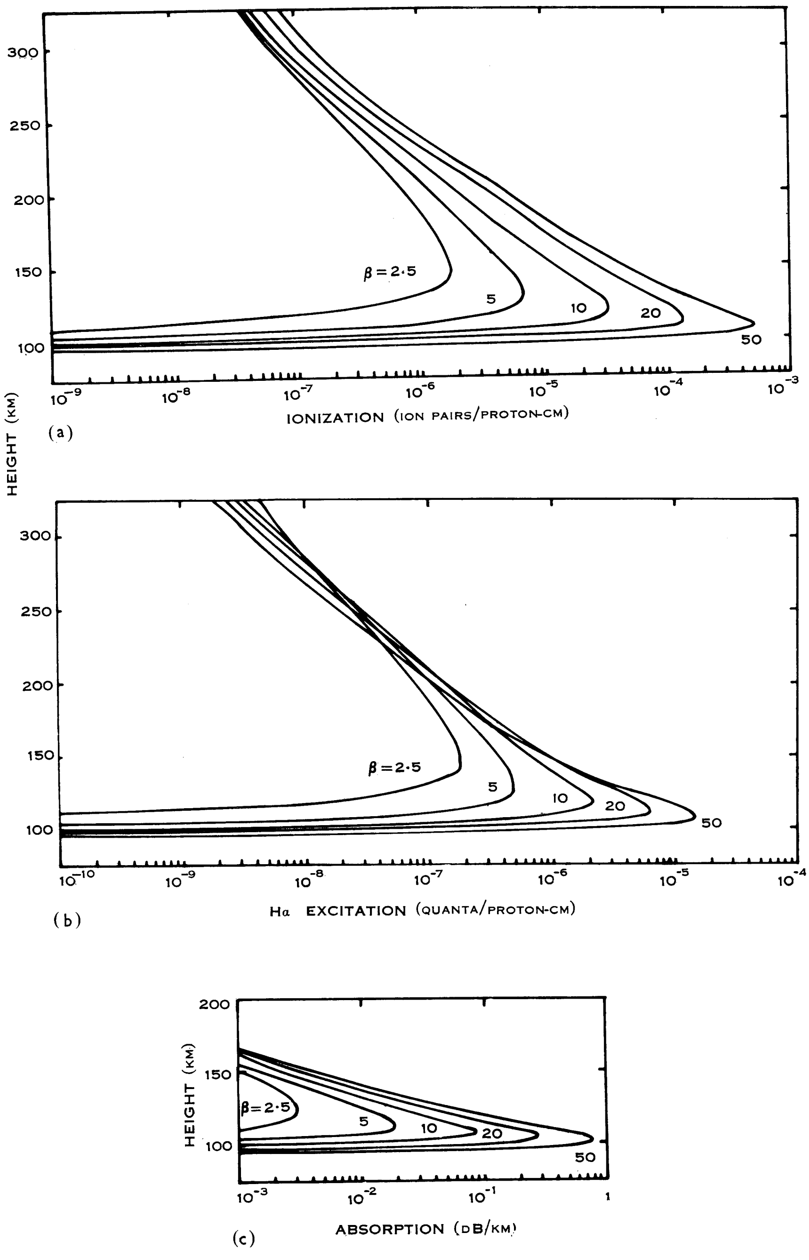

Fig. 8.—Yield profiles for protons distributed in energy according to the initial energy spectra $\exp(-E_0/\beta)$, with 1 keV $\leqslant E_0 \leqslant$ 1 MeV; isotropic angular distribution. (*a*) ionization; (*b*) Hα excitation; (*c*) absorption at 27·6 MHz for an assumed proton flux 10^6 cm^{-2} sec^{-1} sr^{-1}.

Figure 4 shows results of range–energy determinations for protons in air (Jesse and Sadauskis 1950; Cook, Jones, and Jorgenson 1953; Reynolds *et al.* 1953).

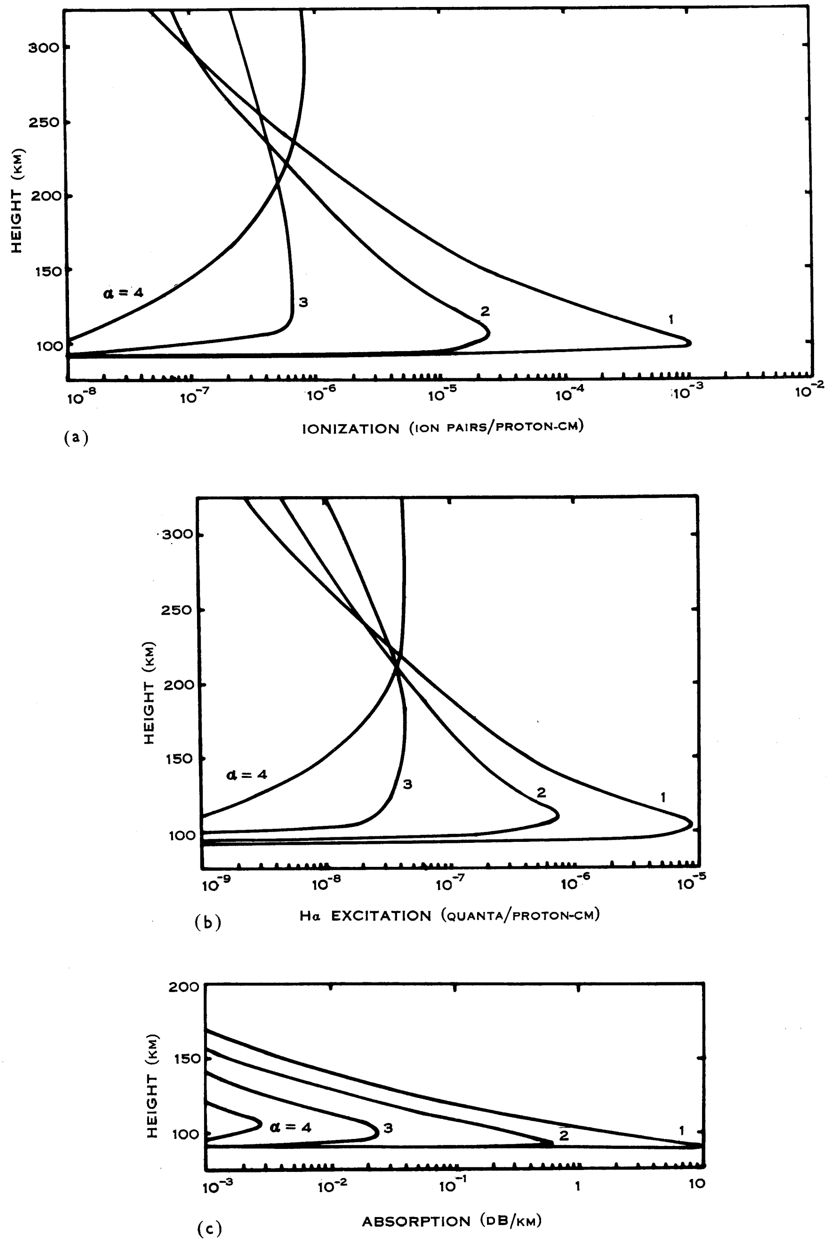

Fig. 9.—Yield profiles for protons distributed in energy according to the initial energy spectra $E_0^{-\alpha}$, with 1 keV $\leqslant E_0 \leqslant$ 1 MeV; isotropic angular distribution. (*a*) ionization (distribution (v) of Section VI used for $\alpha = 1$); (*b*) Hα excitation; (*c*) absorption at 27·6 MHz for an assumed proton flux 10^6 cm^{-2} sec^{-1} sr^{-1}.

The curve drawn through these experimental points has been used here, including an extrapolation from the 6 keV value of $r = 0 \cdot 01$ atm-cm to pass through $r = 0$ at zero energy.

VIII. Computations

The theoretical and empirical relations described above were used to calculate ionization rate, excitation of Hα, and radio absorption at 27·6 MHz, for 20 different heights in the model atmosphere between 90 and 300 km, using the several proton energy spectra described in Section VI. The effects of different pitch-angle distributions were determined for 30 keV monoenergetic incident protons and for a proton energy spectrum varying as $\exp(-20r_0)$. The results, obtained by numerical integrations on CDC 3200 and CDC 3600 computers, are presented in Figures 5–9.

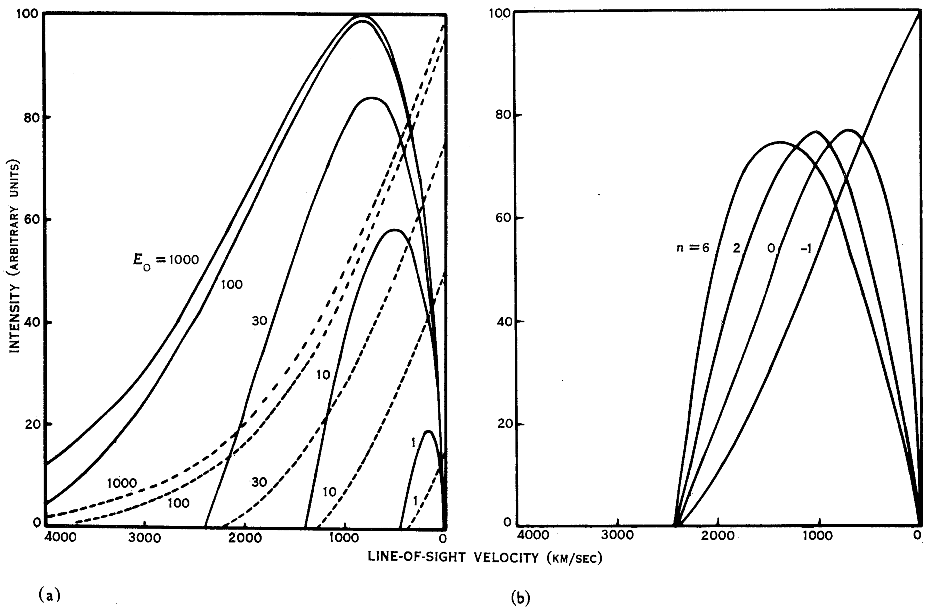

Fig. 10(a).—Theoretical Hα profiles for monoenergetic protons of initial energy E_0 keV, with 1 keV $\leqslant E_0 \leqslant$ 1 MeV; isotropic pitch-angle distribution. ——— magnetic zenith profile; - - - - - magnetic horizon profile.

Fig. 10(b).—Effect of pitch-angle distribution on the theoretical Hα profile for 30 keV protons. The angular distribution parameter n is as defined by equation (1).

Figure 10(a) shows theoretical Hα line profiles, in the magnetic zenith and horizon directions, for monoenergetic protons with isotropic pitch distributions. The effect on the magnetic zenith line profile of varying the pitch-angle distribution is shown in Figure 10(b) for 30 keV protons. Figures 11(a) and 11(b) show theoretical Hα line profiles for exponential and power-law energy distributions respectively. Absolute values obtained may vary by as much as three- or four-fold, due to inaccuracies in the data adopted for electron collision frequency, attachment, and recombination, and to departures from the conditions of the chosen model atmosphere. However, the form of response of excitation and ionization to changes in postulated proton flux parameters is virtually unaffected by these uncertainties.

IX. Discussion

The few rocket measurements of auroral proton energy spectra are summarized in Table 1 of Eather and Jacka (1966*a*). Only the higher energy component of the proton flux was sampled in these flights. However, these high energy observations

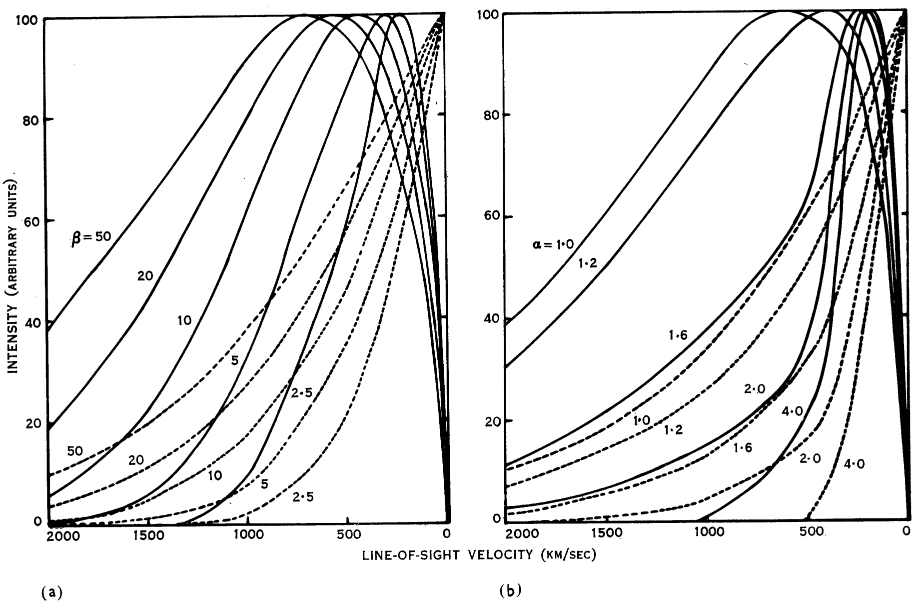

Fig. 11.—Normalized Hα profiles for protons distributed in energy according to the initial energy spectra (*a*) $\exp(-E_0/\beta)$, (*b*) E_0^{-a}, with 1 keV $\leqslant E_0 \leqslant$ 1 MeV; isotropic angular distribution. ——— magnetic zenith profile; - - - - - magnetic horizon profile.

and the calculated absorption curves presented here together indicate that proton precipitation could, at times, cause appreciable absorption of cosmic radio noise at riometer frequencies (see Eather and Jacka 1966*a*).

The computed Hα line profiles (Fig. 10) have been compared with reported observed profiles (summarized by Eather and Jacka 1966*b*), yielding the following general conclusions.

(1) The experimental profiles cannot be explained by assuming a monoenergetic proton flux.

(2) The observed magnetic zenith and magnetic horizon profiles are best fitted by assuming a proton energy spectrum either of the form

$$\psi_1(E_0) \propto \exp(-E_0/7)$$

or

$$\psi_2(E_0) \propto E_0^{-1\cdot 4}$$

and an isotropic pitch-angle distribution. Formally similar energy spectra, with slightly larger numerical constants, also fit the zenith profiles satisfactorily, provided a pitch-angle distribution of the form (1) is assumed with $n > 0$. However, these assumptions lead to horizon half-widths that are smaller than those observed.

The calculations show that the forms of Balmer profiles are much less sensitive to the high energy component of the spectrum than is the riometer absorption. Thus, it is not possible to discriminate between the energy spectra ψ_1 and ψ_2 above by reference to the consequent line profiles; yet, for the same overall range of proton energies, the more populous high energy tail of ψ_2 yields absorption, at the riometer frequency, two orders larger than that resulting from ψ_1.

It is not certain, of course, that such a large range of proton energies is properly to be described by a single spectral distribution function. Barcus (1965) and Rosenbery (1965) have recently presented evidence that two different mechanisms of acceleration control the high and low energy components of the auroral electron flux. The same may be true of the proton flux, in which event the correlation between Balmer profiles and proton-induced riometer absorption would depend, primarily, on the coupling between these mechanisms. Further detailed studies of both manifestations of proton precipitation may thus contribute to a better understanding of the acceleration mechanisms.

X. Acknowledgments

We wish to thank Dr. F. Jacka, of the Mawson Institute for Antarctic Research, Adelaide, S. Aust., for valuable advice and discussions concerning this study. One of us (R.H.E.) is indebted to the Australian National Antarctic Research Expedition and to CSIRO for financial support.

XI. References

Aikin, A. C. (1961).—*J. Atmos. Terr. Phys.* **23**: 287.
Barcus, J. R. (1965).—*J. Geophys. Res.* **70**: 2135.
Chamberlain, J. W. (1961).—"Physics of the Aurora and Airglow." (Academic Press: New York.)
Cook, C. J., Jones, E., and Jorgenson, T. (1953).—*Phys. Rev.* **91**: 1417.
Eather, R. H., and Jacka, F. (1966*a*).—*Aust. J. Phys.* **19**: 215.
Eather, R. H., and Jacka, F. (1966*b*).—*Aust. J. Phys.* **19**: 241.
Fejer, J. A. (1955).—*J. Atmos. Terr. Phys.* **7**: 322.
Hanson, W. B. (1961).—"Satellite Environment Handbook." (Stanford Univ. Press.)
Holt, O. (1963).—Norwegian Defence Research Establishment (Kjeller) Report No. 46.
Hultqvist, B. (1964).—*Planet. Space Sci.* **12**: 579.
Jesse, W. P., and Sadauskis, J. (1950).—*Phys. Rev.* **78**: 1.
Nicolet, M. (1959).—*Physics Fluids* **2**: 95.
Omholt, A. (1956).—*J. Atmos. Terr. Phys.* **9**: 18.
Ratcliffe, J. A., and Weekes, K. (1961).—"Physics of the Upper Atmosphere." (Academic Press: New York.)
Reynolds, H. K., Dunbar, R. D. N. F., Wenzel, W. A., and Whaling, W. (1953).—*Phys. Rev.* **92**: 742.
Rosenbery, T. J. (1965).—*J. Atmos. Terr. Phys.* **27**: 751.